Nat. Hazards Earth Syst. Sci. Discuss., 2, 3935–3963, 2014
www.nat-hazards-earth-syst-sci-discuss.net/2/3935/2014/
doi:10.5194/nhessd-2-3935-2014

Natural Hazards and Earth System Sciences
Discussions
Open Access

Identification of storm surge events over the German Bight from atmospheric reanalysis and climate model data

D. J. Befort[1,2], **M. Fischer**[1], **G. C. Leckebusch**[2,1], **U. Ulbrich**[1], **A. Ganske**[4], **G. Rosenhagen**[3], **and H. Heinrich**[4]

[1]Institute of Meteorology, Freie Universität Berlin, Germany
[2]School of Geography, Earth and Environmental Sciences, University of Birmingham, UK
[3]Deutscher Wetterdienst (DWD), Hamburg, Germany
[4]German Maritime and Hydrographic Agency (BSH), Hamburg, Germany

Received: 17 April 2014 – Accepted: 9 May 2014 – Published: 4 June 2014

Correspondence to: D. J. Befort (daniel.befort@met.fu-berlin.de)

Published by Copernicus Publications on behalf of the European Geosciences Union.

Abstract

A new procedure for the identification of storm surge situations for the German Bight is developed and applied to reanalysis and global climate model data. This method is based on the empirical approach for estimating storm surge height using information about wind speed and wind direction. Here, we hypothesize that storm surge events are caused by 10 m winds with high wind speed and north-westerly direction in combination with a large-scale wind storm event affecting the North Sea region. The method is calibrated for ERA-40 data, using the data of the storm surge atlas for Cuxhaven. It is shown that using information of both: wind speed and direction as well as large-scale wind storm events improves the identification of storm surge events.

To estimate possible future changes of potential storm surge events, we apply our approach to a small ensemble of three transient climate change simulations which are performed with the ECHAM5/MPIOM model under past and A1B greenhouse gas scenario forcing. We find an increase of the total number of storm surge relevant events by about 12 % regarding the ensemble mean for the period from 2001 to 2100 with respect to the period from 1901 to 2000. Yearly numbers of storm surge relevant events show high interannual and decadal variability and only the time series for one of three runs shows a statistical significant increase of the yearly number of storm surge relevant events between 1900 and 2100. However, no changes in the maximum intensity and duration of these events is determined.

1 Introduction

Storm surges over the German coast have a high socio-economic impact, as they are the most dangerous hazard for the coastal areas, even affecting the densely populated metropolitan region of Hamburg.

The factors influencing storm surges are summarized in Weisse et al. (2012) and the knowledge about past and possible future changing storm-surge statistics is reviewed

NHESSD
2, 3935–3963, 2014

in von Storch and Woth (2008). Winds blowing from offshore directions cause a rise of water levels at the coast, which is in particular relevant during high tides. Other factors influencing the rise of the water level during a storm are e.g., local water depth and external surges (Tomczak, 1960; Gönnert and Sossidi, 2011a, b).

The height of a storm surge is defined by the rise of the water level above the mean high water level (MHW). Following the definition used by the German Maritime and Hydrographic Agency (BSH) a storm surge event at the German North Sea coast with water levels exceeding the MHW by 1.5 to 2.5 m is called a "storm surge", an excess of 2.5 to 3.5 m is defined as a "heavy storm" surge and an event exceeding 3.5 m above MHW is called a "very heavy storm surge" (Müller-Navarra et al., 2012). The shape of the German Bight coastline and its estuaries intensifies the water rise as water that is pushed by north-western winds into the southern North Sea is impounded.

The BSH uses dynamical atmospheric and hydrological models to forecast water levels for the German coasts and estuaries. Lately, a dynamical-statistical forecasting system was developed (Müller-Navarra et al., 2012). However, until recently, the forecasts were based on an empirical-statistical approach using a multi-linear regression (Müller-Navarra et al., 2003). The formula used in the latter procedure is based on 13 linear equations using wind speed and wind direction, surface pressure and its change in time, air/water temperature and observed water level in Wick (Scotland) as input data. The factors explaining most of the variability according to these calculations are wind speed and wind direction. Other statistical analysis revealed that the gauges along the German Bight show maximum water level raise by wind when the direction is between 295 and 315°, depending on the individual location. Regional differences in the shape of the coast or the water depth are assigned to the small variations of the optimal wind direction. The optional wind direction of 295°, found out for the town of Cuxhaven, in the center of the German Bight coast, is commonly used as a proxy for the whole region. The component of the observed wind projected on this direction is called the "effective wind" subsequently. The raise to the water level during storm

NHESSD
2, 3935–3963, 2014

surges is determined either by mean sea level changes or changes in wind storm frequency and/or intensity, with only the latter affecting surge height.

Dangendorf et al. (2013) found in an analysis of sea level data from 13 gauges in the German Bight that linear extreme sea level trends exceeded mean sea level trends in the second half of the 20th century, indicating that changes in local extreme winds have played an important role in the recent past. Several recent studies on changes of storm surges under future greenhouse gas (GHG) conditions found only minor or no significant changes for the German and Dutch North Sea coastline (Sterl et al., 2009; Debernard and Roed, 2008; Gaslikova et al., 2012; von Storch and Reichardt, 1997). Other studies found indications of an increase of storm surge extremes at the North Sea coast associated with increased GHG concentrations (Woth et al., 2006; Langenberg et al., 1999). This is in line with Gaslikova et al. (2011), who calculated an increase of insurable losses due to storm surges under future climate scenarios for this regions. With respect to wave heights under scenario conditions Grabemann and Weisse (2008) pointed at increasing extreme wave heights over large parts in the southern and eastern North Sea. This is not a contradiction to findings of de Winter et al. (2012), who found no significant change of projected mean wave heights and periods along the Dutch coasts as there can be different trends in the means and the extremes of an atmospheric phenomenon (see e.g., Ulbrich et al., 2009, 2013; Pinto et al., 2007).

We do not attempt to review the reasons for the different results obtained, in detail. Rather, we develop a new methodology for estimating changes of storm surge risks for the German Bight region solely due to changes in frequency and strength of storms under future climate scenario conditions. It is designed to be used with coarse grid data, meeting the current standard of GCM runs in CMIP5. In a first step, the skill of our method is tested by identifying historic storm surge events in reanalysis data. In a second step, we apply the method to the output data of the GCM IPCC-AR4 ECHAM5/MPIOM ensemble simulations under recent and future climate conditions as the requirement of available zonal and meridional wind data at 6 hourly time steps is

NHESSD
2, 3935–3963, 2014

fulfilled by this model. To estimate the total future storm surge risk in the German Bight, these results can be used to find single events for which corresponding water levels can be calculated and analyzed with regional hydrodynamic models. That means, that we split the future storm surge risk into an atmospheric and an oceanic part and neglect nonlinear interactions of the atmosphere and the ocean.

2 Data

For this study we use the storm surge atlas of the station Cuxhaven (Gönnert and Buß, 2009) covering the period 1901–2008. It comprises a total of 166 storm surges with information about the measured total water level, the calculated astronomical tide and the wind surge. The wind surge height was computed by subtracting total calculated water height and astronomical tide, thus any other factors like external surges have been neglected. The storm surge atlas only includes those storm surge events for which water levels exceeded the MHW by at least 1.5 m. The temporal resolution of time series for total water level, astronomical tide and wind surge is five minutes.

For the calibration of the storm identification method we use the reanalysis data of ERA-40 (Uppala et al., 2005). It covers the period 1957–2002 with a horizontal resolution of 1.125° (≈ 125 km; T159). In this investigation, the zonal and meridional surface wind in 10 m height with a time resolution of 6 h are analyzed.

In order to estimate changes of storm surge risk, the IPCC-AR4 ensemble simulations of the global coupled atmosphere-ocean model ECHAM5/MPIOM with a horizontal resolution of 1.875° (≈ 210 km; T63) are used. In this study, we investigate the three transient ensemble simulations driven with observed GHG forcing for the period 1900 until 2000 (Röckner et al., 2006d, a; Röckner, 2004b) and A1B scenario forcing for the period 2001 until 2100 (Röckner, 2004a; Röckner et al., 2006b, c).

NHESSD
2, 3935–3963, 2014

3 Method

An identification of all wind events potentially leading to extreme storm surges along the German Bight coast is hindered by coarse resolution of the global climate model simulations in which the German Bight region is represented by about two grid boxes only. Wind speed data from these grid points may not be representative for a situation with a major surge-producing storm, potentially including some small and short lasting events.

In this study, we investigate the improvements of the identification of past storm surge events by additionally comprising the large scale wind field over the North Sea region. The gain of this procedure is investigated in Sect. 4.1.

3.1 Effective wind speed

As the basis for the identification of storm surge events we apply the statistical approach developed by the German Maritime and Hydrographic Agency (Müller-Navarra et al., 2003). It considers the effective wind, which is the projection of wind speeds on the direction of 295° (WNW direction). In this study, we use the mean effective wind speed calculated using all gridpoints within the German Bight region, which consists of seven grid boxes in ERA-40 reanalysis data and two grid cells in ECHAM5 model data (Fig. 1a and b).

3.2 Wind storm identification

Our identification of large-scale wind storms is based on the methodology described by Leckebusch et al. (2008). This algorithm uses the surface wind speed in a dataset, looking for spatially coherent regions with grid points exceeding the local 98th percentile of absolute wind speed for each model time step. Such a storm region is a candidate for a wind storm event if it has a minimum area of about 150 000 km^2 ($\approx$ 20 (7) grid points in ERA-40 (ECHAM5) at 60° N). As it may occur that a wind field cluster with grid boxes

NHESSD
2, 3935–3963, 2014

exceeding the 98th percentile is decomposed into subcluster where none of these fulfill the minimum size required, we use an envelope constructed of the 95th percentile. Thus, even if none of the individual subcluster match the size criterion solely, it will be counted as a candidate for a wind field track, if those subclusters are connected through the 95th percentile and the total size of all these subclusters exceed the minimum area. These identified clusters are tracked in time using a nearest-neighbor algorithm. Two wind fields are, however, not linked if a maximum distance is exceeded. The distance includes a fixed part of 600 km and the half of the storm area. Eventually, storm events must have a minimum duration of 18 h.

During the period covered by ERA-40 reanalysis data (1957–2002) 83 storm surges are observed, whereof 82 occurred in the winter season (September until May). Thus, our analysis focuses on the months September until May as this is the primary season for strong storm surges in the German Bight area.

Using ERA-40 reanalysis data we calculate the 98th percentile of 10 m wind speed over the whole period from 1957 until 2002. To estimate changes in storm surge potential the 98th percentile for ECHAM5 is calculated using all three ensemble members from the 20C simulations only. This percentile is used for the detection of storm events during 1900 until 2000 regarding 20C period and 2001 until 2100 for ECHAM5 A1B scenario period, respectively.

3.3 Method to detect storm surge relevant events

In this study, we use both criteria explained above to detect storm surge relevant events. Thus, an event with storm surge potential is characterized by their mean effective wind speeds over the German Bight region (see Sect. 3.1) and a large-scale wind storm event, detected by the algorithm explained (see Sect. 3.2) in the vicinity of the German North Sea coast.

Events are only considered if the large-scale wind storm is located over parts of the North Sea region. This region is illustrated in Fig. 1a and b for ERA-40 reanalysis and

NHESSD
2, 3935–3963, 2014

ECHAM5 model grids, respectively. In total, the region consists of 99 grid boxes in ERA-40 and 35 grid boxes in ECHAM5.

4 Results

The analysis is divided into four parts. In a first step, we apply the method developed by BSH to detect storm surge relevant situations using effective wind speed data calculated from ERA-40 reanalysis data (Uppala et al., 2005) over the German Bight solely. Using the storm surge catalog from the station Cuxhaven (Gönnert and Buß, 2009) we assign storm surge events to their effective wind speeds. Secondly, we use the new method presented in Sect. 4.1, combining effective wind speed information and large-scale wind storm events to identify storm surge relevant events. Comparing both methods gives an estimate of the additional value of our proposed methodology. In a third step, this approach is transfered to ECHAM5 model data (Röckner, 2004b, a; Röckner et al., 2006a, b, c, d). Detection of potential storm surge events under recent and future climate conditions gives an estimate of the possible changes of storm surge activity over the German Bight region. In a last step, extreme value statistics is applied to the results of the latter section to calculate return levels for these events, followed by a short conclusion and discussion.

4.1 Storm surge events in ERA-40 reanalysis data

As no information about the astronomical tide is included in the IPCC-AR4 ECHAM5/MPI-OM simulations, our analysis is based on wind speed and wind direction only. Thus, we use the wind surge data from the storm surge catalog at the station in Cuxhaven only, neglecting the influences of the water depths or the astronomical tide.

Our first attempt in identifying storm surge relevant events in atmospheric model data is based on an empirically derived relationship between surge and wind, deviated from observed wind and surge data at BSH. First, we calculate effective wind speed over the

NHESSD
2, 3935–3963, 2014

German Bight every six hours from ERA-40 reanalysis data. Afterwards, we determine the dates of observed storm surge events from the storm surge atlas of Cuxhaven. As we focus on wind surge height, the date assigned to an observed storm surge event is the one at wind surge maximum. As the storm surge atlas gives information about wind surge every 5 min, but as wind data is only available on a six hourly time scale in ERA-40, we take for the height of the respective surge both dates before and after wind surge maximum, into account. To estimate the usability of this method we calculate the ratio between the number of time steps in ERA-40 reanalysis data which are assigned to an observed storm surge and the total number of time steps exceeding the minimum effective wind speed during an observed storm surge. We calculate a ratio of about 3.7 %.

As our proposed method is based on the combination of high effective wind speeds and a large-scale wind storm event, we first identify large-scale storm events with a minimum duration, size and strength in ERA-40 data (see Sect. 3). In total, 3541 events are found during the winter season for the period 1957 until 2002. This large number is due to the extent of the domain in which wind storm events are identified, covering the whole North Atlantic and Europe. 1353 out of 3541 events have at least one time step with an exceedance of the local 98th percentile over at least one grid box within the North Sea region. As we hypothesize that a large-scale wind storm over the North Sea region is obligatory for the occurrence of a storm surge, only these 1353 are considered.

As expected, not all 1353 wind storm events affecting a North Sea grid point led to a high observed wind surge. We identify those events which are associated with a high wind surge at Cuxhaven by looking for a wind field event which is part of an existing wind storm event affecting the North Sea region at the date of the observed wind surge maximum. If a wind field event can be assigned, the effective wind speed over the German Bight is computed from ERA-40 and assigned to this storm surge event.

There are two possibilities to assign an effective wind from ERA-data to the observed surge maxima. The first idea is to take the higher of the two subsequent (6 hourly)

NHESSD
2, 3935–3963, 2014

values before or after the surge maximum. With this approach a frequency distribution of maximum effective winds can be calculated (Fig. 2a), with those occurring at storm surges according to the Cuxhaven catalog marked in red. Apparently, the catalog suggests that storm surges are characterized by a minimum wind speed of about 9.45 m s^{-1} in reanalysis data over the German Bight region. Note that the maximum effective wind speed is not always found at one of the 6 hourly time steps before or after the maximum surge. One of the reasons for this fact could be related to the actual astronomic tide as the effect of high wind speeds is reduced during high tide compared to low tide (Tomczak, 1960). As well, this minimum effective wind speed value reflects the mean over seven grid boxes in ERA-40 reanalysis data. Therefore, it is smaller than observed wind speeds at a particular station during storm surges.

In a second approach we assign the highest effective wind speed during the whole wind storm event and do not consider only the maximum of the two subsequent values before or after the surge maximum. In this case, the shape of the frequency distribution is slightly changed compared to the first distribution (Fig. 2b). Nevertheless, with this method we find for all storms with effective wind speed larger than 19 m s^{-1} a corresponding storm surge that has been observed at Cuxhaven.

The large number of storms with comparable low effective wind speeds, which could not be assigned to an observed storm surge could be caused by the effect that we neglected the interaction of the tide and the winds. Furthermore, the storm surge catalog from the station Cuxhaven only lists events which led to a minimum total water height of 1.5 m above MHW. Thus, even if a high wind surge is present but it does not occur during a favorable tide phase, this threshold for total water height is not reached and the event is not included in the storm surge catalog. Events with effective wind speeds larger than 19 m s^{-1} cause a very high wind surge, thus leading to a storm surge independently of the astronomical tide.

Similar to the first approach based on effective wind speed data only, we calculate the ratio between those observed storm surge events which can be assigned to a large scale wind storm track and all time steps of the ERA-40 period which are characterized

NHESSD
2, 3935–3963, 2014

by a large-scale wind storm event over the North Sea region in combination with an effective wind speed exceeding 9.45 m s^{-1}. This ratio is about 5.5 %, but it should be also mentioned that two out of 82 observed storm surge events cannot be assigned to a large-scale wind storm event. One of these events is characterized by a too short large-scale wind storm event, lasting only two time steps. In the second case, two separated wind fields exist whereof one is located over the North Sea and the other one is located over Scandinavia. Due to the simple nearest neighbor algorithm the wind field over Scandinavia is connected to the existing wind storm event as it is closer to the previous wind field, and the wind field over the North Sea is neglected.

Overall, the approach based on the combination of high effective wind speeds and large-scale wind storm events over the North Sea region outperforms the approach based on effective wind speeds solely, which makes this method well suited for coarse resolved GCM data.

4.2 Potential storm surge events in ECHAM5 20C and A1B

To identify storm surge relevant events in ECHAM5 model data, we apply some minor changes to the method presented in Sect. 4.1. This is explained by a coarser spatial resolution of the GCM data with 1.875° compared to 1.125° in ERA-40 reanalysis data. Thus, the regions for the German Bight and North Sea used for the identification in ECHAM5 are not the same regions used in ERA-40. Section 4.1 shows that storm surge events do occur when the spatial mean of the ERA-40 effective wind speed over the German Bight exceeds 9.45 m s^{-1} in combination with a large-scale storm field over the North Sea region. As absolute wind speeds can essentially differ between spatially lower resolved model and reanalysis data, we use percentile values rather than absolute wind speed values. An effective wind speed of 9.45 m s^{-1} in ERA-40 reanalysis data corresponds to a percentile value of 91.97 %.

Thus, a potential storm surge event identified in ECHAM5 data is characterized by a large-scale wind field over the North Sea region and an effective wind speed over the German Bight exceeding the 91.97th percentile. The 91.97th percentile of effective

NHESSD
2, 3935–3963, 2014

wind speed over the German Bight in ECHAM5 data corresponds to an absolute wind speed of 9.84 m s^{-1}. To calculate this value we use the 20C realizations solely. As explained in Sect. 3 the threshold obtained from the 20C data is also used for the identification of potential storm surge events in ECHAM5 A1B model data.

4.2.1 Number of potential storm surge events

The number of events within the whole identification area covering most of the North Atlantic is statistically significant lower during the A1B period with respect to the 20C period (see Table 1). However, the increased number of events with at least one time step within the North Sea region during the A1B period could indicate a shift of the cyclone tracks. Considering the sum of all three ensemble members of the 20C and A1B period, we find an increase of potential storm surge events affecting the North Sea region (with effective wind speed above 9.84 m s^{-1}) by 12.4 % in A1B compared to 20C.

The annual numbers of potential storm surge events for all three ensemble members for the period 1900 until 2100 is shown in Fig. 3. The ensemble mean of the ensemble members (black squares) of the 20C scenario (green to blue) and the A1B scenario (yellow to red) reveals a statistical significant linear trend with an error probability of $\alpha = 0.01$ and an increase in storm surge relevant events of almost 1.5 events within the period 1900–2100. By considering the three runs separately, the relevance of the simulated decadal climate fluctuations are shown: run 1 offers a significant increase of almost 3 events in 200 years with an error probability of $\alpha = 0.001$. In run 2, a rise is seen as well, which however is not statistical significant. Run 3 shows a slight decrease, which is also not statistical significant. However, taken into account the large interannual fluctuations in the range between 2 and 28 events per year, the increase of even 3 events in 200 years is very moderate.

In Fig. 4 the 30 year moving mean of the number of potential storm surge events per year for the considered runs and for whose mean values is plotted. The large decadal fluctuations can be clearly seen in the time series of the means. Therefore, it has to

NHESSD
2, 3935–3963, 2014

be noted that the increase numbers of relevant storms is not monotonic. As well, the 30 years periods with the largest numbers of storm surge relevant events are not found at the end of the 21st century for all three ensemble members.

We calculate the exceedance of the threshold of 9.84 m s^{-1} for each storm in 20C and A1B to investigate if the total increase of these events is valid independently from its severity (Fig. 5, Table 2). For the majority of classes the number of storm events in A1B has increased with respect to those of the 20C simulations. A high increase of at least 10 % occurs for exceedings of 2–7 m s^{-1}. Particularly, extreme events with exceedings of 11–12 and 13–14 m s^{-1} over the threshold of 9.84 m s^{-1} become frequent, whereas the number of events with effective wind speed of 20.84 to 21.84 m s^{-1} increased by nearly 130 % when considering the overall frequency-distribution (Table 2). However, the storms with exceedings of 8–11 and 12–13 m s^{-1} become infrequent for the A1B runs. This could be an indication for a shift of moderate extreme events to heavy extreme events. For storms with an exceedance of 14 m s^{-1} and more the percentage changes are insignificant due to the low numbers of events. A Pearson's chi-squared-test with a error probability of $\alpha = 0.05$ reveals that the distributions arise from the same population.

4.2.2 Duration of potential storm surge events

In addition to the number of potential storm surge events we investigate if the duration of such events changes under future conditions. Therefore, the number of time steps are counted for which the storm is located in the region of the North Sea and the effective wind speed of 9.84 m s^{-1} is exceeded. An increased storm surge potential can be assumed due to an increased duration of the events, even if the maximum effective wind speed is unchanged. Figure 6 depicts the percentage of exceedings for the runs of 20C and A1B with respect to the total number of tracks in the respective century. However, a Pearson's chi-squared-test of the distributions of 20C and A1B with a error probability of $\alpha = 0.05$ shows no evidence for a change of the duration.

NHESSD
2, 3935–3963, 2014

4.2.3 Return levels of extreme effective wind speed

To investigate the occurrence rate of extreme events the extreme value statistics (EVS) provides a suitable approach. At this point, only the basic idea of the theory is covered and reference is made to more in-depth literature, e.g. Coles (2001). In EVS extreme values above a certain threshold can be described by using the Generalized Pareto Distribution (GPD) given by:

$$H(y) = 1 - \left(1 + \frac{\xi y}{\tilde{\sigma}}\right)^{-1/\xi} \quad \text{with } \{y : y > 0\}, (1 + \xi y/\tilde{\sigma}) > 0$$

with the form parameter, ξ, and the scale parameter, σ, which is in linear relationship to a statistical threshold value used for restricting the assessment to extremes. Low values in a distribution are not used in the GPD. The choice of the statistical threshold is delicate as if the threshold is chosen to high, there exist not enough values for the statistical analysis. For the peak over threshold approach a selection of an appropriate threshold, u, is vital. Guidance for threshold selection is provided by the mean residual life plot (mrlp); if the threshold u_0 is large enough to ensure the GPD approximation to be valid then, for all thresholds $u > u_0$, a linear relationship between the mean of excesses $(x - u|x > u)$ and the threshold u holds.

The mrlp derived by using all three 20C ensemble members is shown in Fig. 7. In addition to the mean excess (continuous line) their 95 % confidence interval is drawn as well (dotted lines). The red vertical line marks the threshold of 9.84 m s^{-1} derived from historical storm surges (cf. Sect. 4.2) with more than a quarter of the time steps exceeding that threshold. However, based on the mrlp, this threshold is too low to allow for a reliable approximation with the GPD; the plot rather suggest a threshold of 18.0 m s^{-1}. With this threshold we calculate return levels using all three ensemble members available during A1B and the 20C period (Fig. 8). In this case the return levels specify the effective wind speed in m s^{-1} which is expected to be exceeded on average once in a certain return period. As expected, the increased amount of

NHESSD
2, 3935–3963, 2014

potential storm surge events is also reflected in slightly raised return levels on the interannual to interdecadal scale (return levels 0.1–7) for the runs of A1B. The effective wind speeds which are expected to be exceeded several times a year are increased by nearly 0.5 m s^{-1} in the A1B runs with respect to 20C. On the decadal to multi-decadal scale the return levels are higher for 20C because of a few more events of the strongest intensity classes (Fig. 5). The increased uncertainty of the multi-decadal return levels are expressed by bigger confidence intervals.

5 Conclusions

In this study, changes of the storm surge risk at the German Bight coasts caused by possible changes of meteorological parameters under future climate conditions are investigated. In order to detect storm surge events in meteorological reanalysis and climate model data, we use surface wind vectors only. We hypothesize that storm surge events are attributed to strong near surface wind speeds over the German Bight projected on a wind direction of 295°, as well as a large-scale wind storm event affecting the North Sea region.

Using ERA-40 reanalysis data and the storm surge atlas for the station Cuxhaven, 80 out of 82 observed storm surge events between September and May could be assigned to a large-scale wind storm event. The reason that two events could not be assigned to any event is mainly due to difficulties to detect smaller wind storms or very intense wind storms, which move very fast through the North Sea region within few hours. These smallest wind storms could not be detected by the algorithm which is based on a simple nearest neighbor approach.

Our analysis shows that storm surge events are characterized by an effective wind speed exceeding 9.45 m s^{-1} in ERA-40, but not every wind event with an effective wind speed over 9.45 m s^{-1} leads to an observed storm surge. This is mainly explained by the fact that tides are not taken into account in our approach. As the interaction of tides and high winds are important for the development of a storm surge, it can also

NHESSD
2, 3935–3963, 2014

be observed that not every storm causes a storm surge. Nevertheless, if the effective wind speed is high enough, then water levels rise above the criterion height for storm surges, independent of the phase of the tide. In these cases, the respective tidal phase only determines the severeness of the storm surge. For ERA-40 winds, all wind storm events with effective wind speeds exceeding 19 m s^{-1} can be attributed to an observed storm surge.

We show the relevance of not using local effective winds only to detect storm surge relevant events in gridded datasets. We determine an additional value of our method combining effective wind speed data and large-scale wind storm events compared to the method using effective wind speed data solely.

We apply our methodology to three runs of the ECHAM5/MPI-OM simulations forced by observed greenhouse gas concentrations (GHG) for the period 1900 until 2000 and with GHG concentrations following the SRES A1B scenario from 2001 until 2100. As absolute wind speed distributions between model and reanalysis data differ, we use an effective wind speed of 9.84 m s^{-1} for ECHAM5 data, corresponding to the same percentile value of 91.97 % as 9.45 m s^{-1} in ERA-40.

The total number of potential storm surge events identified in all three runs under the A1B scenario for the whole period between 2001 and 2100 is increased by 12,4 % with respect to the 20C period (1901–2000). All three time series of yearly numbers of potential storm surge events display a high interannual and decadal variability. Only one simulation shows a significant increase of the number of potential storm surge events per year, while the two others show either an increasing or a decreasing trend, which are both not significant. We find no changes in the strength of the most violent effective winds as well as in the duration of potential storm surge events.

Extreme value statistics reveals an increase of events with a 3–4 year return period, whereas the multi-decadal events exhibit lower effective wind speeds. However, confidence intervals for high return levels are large.

NHESSD
2, 3935–3963, 2014

Acknowledgements. The authors thank the LSBG (Landesbetrieb für Straßen, Brücken und Gewässer) in Hamburg for providing data from the storm surge atlas for the station Cuxhaven as well as ECMWF for providing ERA-40 reanalysis data. This work was funded by the KLIWAS research programme of the Federal Ministry of Transport and Digital Infrastructure (BMVI).

References

Coles, S.: An Introduction to Statistical Modeling of Extreme Values, Springer-Verlag, London, 2001. 3948

Dangendorf, S., Mudersbach, C., Jensen, J., Ganske, A., and Heinrich, H.: Seasonal to decadal forcing of high sea level percentiles in the German Bight throughout the last century, Ocean Dynam., 63, 533–548, 2013. 3938

Debernard, J. B. and Roed, L. P.: Future wind, wave and storm surge climate in the Northern Seas: a revisit, Tellus A, 60, 427–438, 2008. 3938

de Winter, R., Sterl, A., de Vries, J. W., Weber, S. L., and Ruessink, G.: The effect of climate change on extreme waves in front of the Dutch coast, Ocean Dynam., 62, 1139–1152, 2012. 3938

Gaslikova, L., Schwerzmann, A., Raible, C. C., and Stocker, T. F.: Future storm surge impacts on insurable losses for the North Sea region, Nat. Hazards Earth Syst. Sci., 11, 1205–1216, doi:10.5194/nhess-11-1205-2011, 2011. 3938

Gaslikova, L., Grabemann, I., and Groll, N.: Changes in North Sea storm surge conditions for four transient future climate realizations, Nat. Hazards, 66, 1501–1518, 2012. 3938

Gönnert, G. and Buß, T.: Sturmfluten zur Bemessung von Hochwasserschutzanlagen, Landesbetrieb Straßen, Brücken und Gewässer, Hamburg, 2009. 3939, 3942

Gönnert, G. and Sossidi, K.: A new approach to calculate extreme storm surges: analysing the interaction of storm surge components, in: Coastal Processes II, Vol. 149, 139–150, WIT PRESS, Southhampton, 139–150, 2011a. 3937

Gönnert, G. and Sossidi, K.: A new approach to calculate extreme storm surges, Irrig. Drain., 60, 91–98, 2011b. 3937

Grabemann, I. and Weisse, R.: Climate change impact on extreme wave conditions in the North Sea: an ensemble study, Ocean Dynam., 58, 199–212, 2008. 3938

NHESSD

2, 3935–3963, 2014

Langenberg, H., Pfizenmayer, A., von Storch, H., and Sundermann, J.: Storm-related sea level variations along the North Sea coast: natural variability and anthropogenic change, Cont. Shelf Res., 19, 821–842, 1999. 3938

Leckebusch, G., Renggli, D., and Ulbrich, U.: Development and application of an objective storm severity measure for the Northeast Atlantic region, Meteorol. Z., 15, 575–587, 2008. 3940

Müller-Navarra, S. H., Lange, W., Dick, S., and Soetje, K. C.: Über die Verfahren der Wasserstands- und Sturmflutvorhersage: hydrodynamisch-numerische Modelle der Nord- und Ostsee und empirisch-statistisches Verfahren für die Deutsche Bucht, Promet, 29, 117–124, 2003. 3937, 3940

Müller-Navarra, S. H., Seifert, W., Lehmann, H.-A., and Maudrich, S.: Sturmflutvorhersage für Hamburg 1962 und heute, Bundesamt für Seeschifffahrt und Hydrographie, Hamburg und Rostock, 2012. 3937

Pinto, J. G., Ulbrich, U., Leckebusch, G. C., Spangehl, T., Reyers, M., and Zacharias, S.: Changes in storm track and cyclone activity in three SRES ensemble experiments with the ECHAM5/MPI-OM1 GCM, Clim. Dynam., 29, 195–210, 2007. 3938

Röckner, E.: IPCC-AR4 MPI-ECHAM5_T63L31 MPI-OM_GR1.5L40 SRESA1B run no.2: atmosphere 6 HOUR values MPImet/MaD Germany, World Data Center for Climate (WDCC), 2004a. 3939, 3942

Röckner, E.: IPCC-AR4 MPI-ECHAM5_T63L31 MPI-OM_GR1.5L40 20C3M run no.2: atmosphere 6 HOUR values MPImet/MaD Germany, World Data Center for Climate (WDCC), 2004b. 3939, 3942

Röckner, E., Lautenschlager, M., and Esch, M.: IPCC-AR4 MPI-ECHAM5_T63L31 MPI-OM_GR1.5L40 20C3M run no.3: atmosphere 6 HOUR values MPImet/MaD Germany, World Data Center for Climate (WDCC), 2006a. 3939, 3942

Röckner, E., Lautenschlager, M., and Schneider, H.: IPCC-AR4 MPI-ECHAM5_T63L31 MPI-OM_GR1.5L40 SRESA1B run no.1: atmosphere 6 HOUR values MPImet/MaD Germany, World Data Center for Climate (WDCC), 2006b. 3939, 3942

Röckner, E., Lautenschlager, M., and Schneider, H.: IPCC-AR4 MPI-ECHAM5_T63L31 MPI-OM_GR1.5L40 SRESA1B run no.3: atmosphere 6 HOUR values MPImet/MaD Germany, World Data Center for Climate (WDCC), 2006c. 3939, 3942

Röckner, E., Lautenschlager, M., and Schneider, H.: IPCC-AR4 MPI-ECHAM5_T63L31 MPI-OM_GR1.5L40 20C3M run no.1: atmosphere 6 HOUR values MPImet/MaD Germany, World Data Center for Climate (WDCC), 2006d. 3939, 3942

NHESSD

2, 3935–3963, 2014

Sterl, A., van den Brink, H., de Vries, H., Haarsma, R., and van Meijgaard, E.: An ensemble study of extreme storm surge related water levels in the North Sea in a changing climate, Ocean Sci., 5, 369–378, doi:10.5194/os-5-369-2009, 2009. 3938

Tomczak, G.: Über die Genauigkeit der Sturmflutvorhersage für die deutsche Nordseeküste, Deutsche Hydrografische Z., 13, 1–13, doi:10.1007/BF02224731, 1960. 3937, 3944

Ulbrich, U., Leckebusch, G., and Pinto, J.: Extra-tropical cyclones in the present and future climate: a review, Theor. Appl. Climatol., 96, 117–131, doi:10.1007/s00704-008-0083-8, 2009. 3938

Ulbrich, U., Leckebusch, G. C., Grieger, J., Schuster, M., Akperov, M., Bardin, M. Y., Feng, Y., Gulev, S., Inatsu, M., Keay, K., Kew, S. F., Liberato, M. L. R., Lionello, P., Mokhov, I. I., Neu, U., Pinto, J. G., Raible, C. C., Reale, M., Rudeva, I., Simmonds, I., Tilinina, N. D., Trigo, I. F., Ulbrich, S., Wang, X. L., and Wernli, H.: Are greenhouse gas signals of Northern Hemisphere winter extra-tropical cyclone activity dependent on the identification and tracking algorithm?, Meteorol. Z., 22, 61–68, 2013. 3938

Uppala, S. M., KÅllberg, P. W., Simmons, A. J., Andrae, U., Bechtold, V. D. C., Fiorino, M., Gibson, J. K., Haseler, J., Hernandez, A., Kelly, G. A., Li, X., Onogi, K., Saarinen, S., Sokka, N., Allan, R. P., Andersson, E., Arpe, K., Balmaseda, M. A., Beljaars, A. C. M., Berg, L. V. D., Bidlot, J., Bormann, N., Caires, S., Chevallier, F., Dethof, A., Dragosavac, M., Fisher, M., Fuentes, M., Hagemann, S., Hólm, E., Hoskins, B. J., Isaksen, L., Janssen, P. A. E. M., Jenne, R., Mcnally, A. P., Mahfouf, J.-F., Morcrette, J.-J., Rayner, N. A., Saunders, R. W., Simon, P., Sterl, A., Trenberth, K. E., Untch, A., Vasiljevic, D., Viterbo, P., and Woollen, J.: The ERA-40 re-analysis, Q. J. Roy. Meteorol. Soc., 131, 2961–3012, doi:10.1256/qj.04.176, 2005. 3939, 3942

von Storch, H. and Reichardt, H.: A Scenario of Storm Surge Statistics for the German Bight at the Expected Time of Doubled Atmospheric Carbon Dioxide Concentration, J. Climate, 10, 2653–2662, 1997. 3938

von Storch, H. and Woth, K.: Storm surges: perspectives and options, Sustain. Sci., 3, 33–43, doi:10.1007/s11625-008-0044-2, 2008. 3937

Weisse, R., von Storch, H., Niemeyer, H. D., and Knaack, H.: Changing North Sea storm surge climate: an increasing hazard?, Ocean Coast. Manage., 68, 58–68, 2012. 3936

Woth, K., Weisse, R., and von Storch, H.: Climate change and North Sea storm surge extremes: an ensemble study of storm surge extremes expected in a changed climate projected by four different regional climate models, Ocean Dynam., 56, 3–15, 2006. 3938

NHESSD

2, 3935–3963, 2014

Table 1. Amount of events within the whole identification area (top line), events with at least one time step within the North Sea (NS) region (middle line) and the amount of potential storm surge events (effective wind speed (v_{eff}) above 9.84 m s^{-1} large-scale wind storm affecting North Sea region, bottom line) for each scenario run of ECHAM5 20C (1901–2000) and ECHAM5 A1B (2001–2100).

Data	20C 1	20C 2	20C 3	A1B 1	A1B 2	A1B 3
Total storm events	8801	8823	8811	8305	8327	8353
Events with wind storm over NS	2895	2868	2978	2978	3008	2891
Potential storm surge events wind storm over NS and $v_{eff} > 9.84$ m s^{-1}	961	1008	1072	1142	1202	1075

NHESSD
2, 3935–3963, 2014

Table 2. Percental changes in the number of potential storm surge events of all three ensemble members during 2001–2100 (A1B) compared to the 1901–2000 (20C).

Effective wind speed [m s^{-1}]	Exceeding of the threshold [m s^{-1}]	Increase [%]
9.84–10.84	0–1	5.94 %
10.84–11.84	1–2	9.43 %
11.84–12.84	2–3	18.04 %
12.84–13.84	3–4	18.80 %
13.84–14.84	4–5	15.94 %
14.84–15.84	5–6	16.82 %
15.84–16.84	6–7	11.18 %
16.84–17.84	7–8	9.42 %
17.84–18.84	8–9	−9.52 %
18.84–19.84	9–10	−8.84 %
19.84–20.84	10–11	−7.37 %
20.84–21.84	11–12	126.67 %
21.84–22.84	12–13	−19.35 %
22.84–23.84	13–14	38.46 %
23.84–24.84	14–15	62.5 %
24.84–25.84	15–16	−33.34 %
25.84–26.84	16–17	−50.00 %

NHESSD
2, 3935–3963, 2014

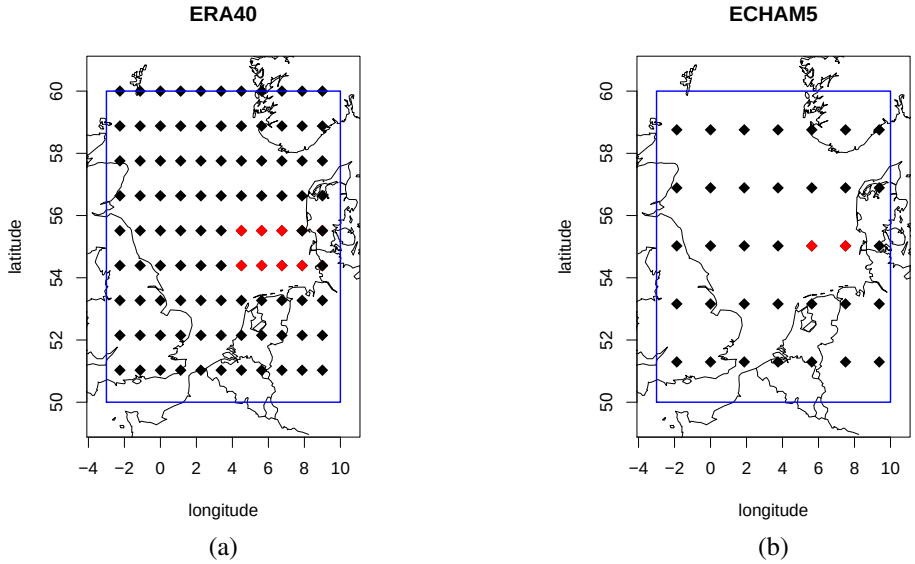

Figure 1. (a) German Bight (red dots) and North Sea region (black dots) for ERA-40 reanalysis, **(b)** German Bight (red dots) and North Sea region (black dots) for ECHAM5 (T63) data.

NHESSD
2, 3935–3963, 2014

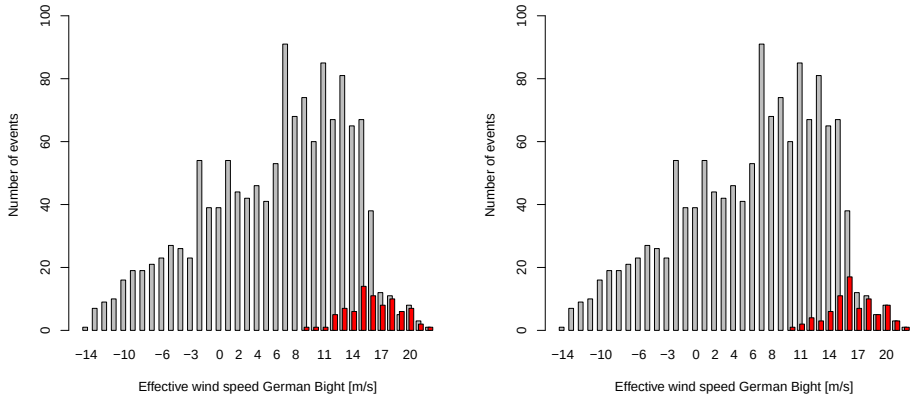

(a) (b)

Figure 2. (a) Histogram of effective wind speed over the German Bight region for all large-scale wind storm events (grey) and wind storm events which could be assigned to an observed storm surge (red). Effective wind speed for assigned events are calculated using the maximum of the ERA-40 time step directly before and after the wind surge maximum.
(b) Same as **(a)** but here effective wind speed for assigned events (red) is calculated using the maximum effective wind speed during the whole large-scale wind storm track.

NHESSD
2, 3935–3963, 2014

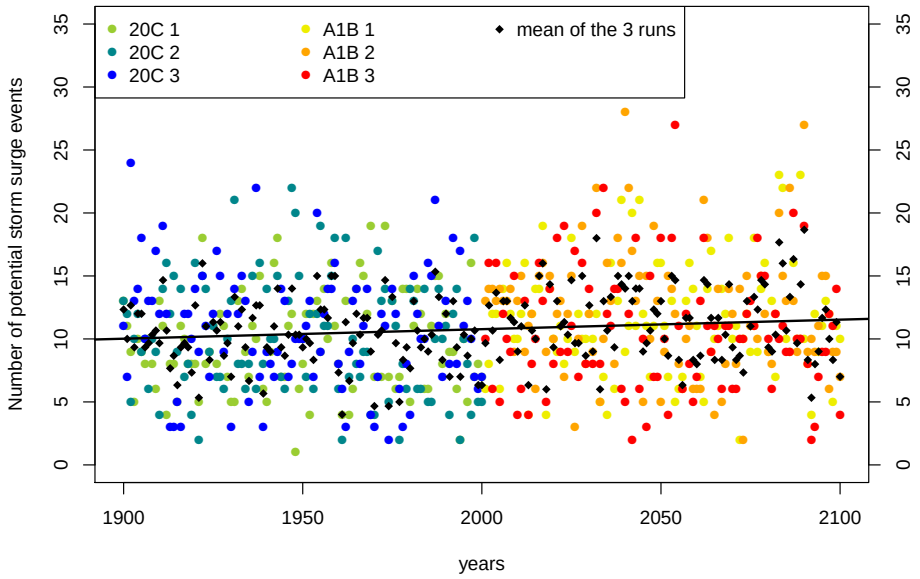

Figure 3. Annual amount of potential storm surge events from 1900 to 2100 for the scenario runs of 20C (green to blue) and A1B (yellow to red). The black squares denote the ensemble mean. The black line marks the statistically significantly linear trend of the ensemble mean with a probability of error of $\alpha = 0.01$.

NHESSD
2, 3935–3963, 2014

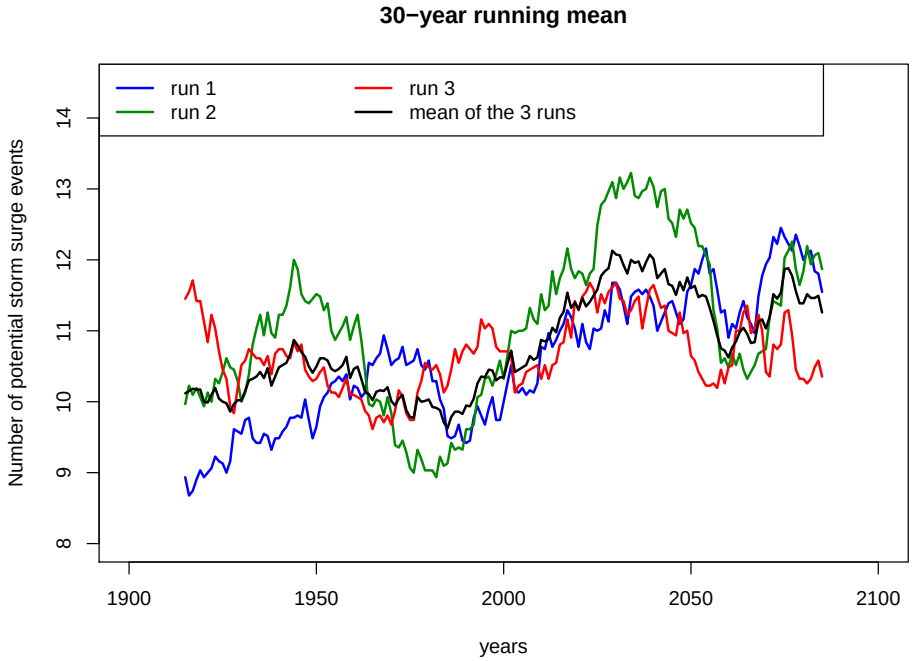

Figure 4. 30 year moving mean of the annual number of potential storm surge events from 1915 to 2085 for the three runs (run 1: blue, run 2: green, run 3: red) and for the mean of all ensemble members (black).

NHESSD
2, 3935–3963, 2014

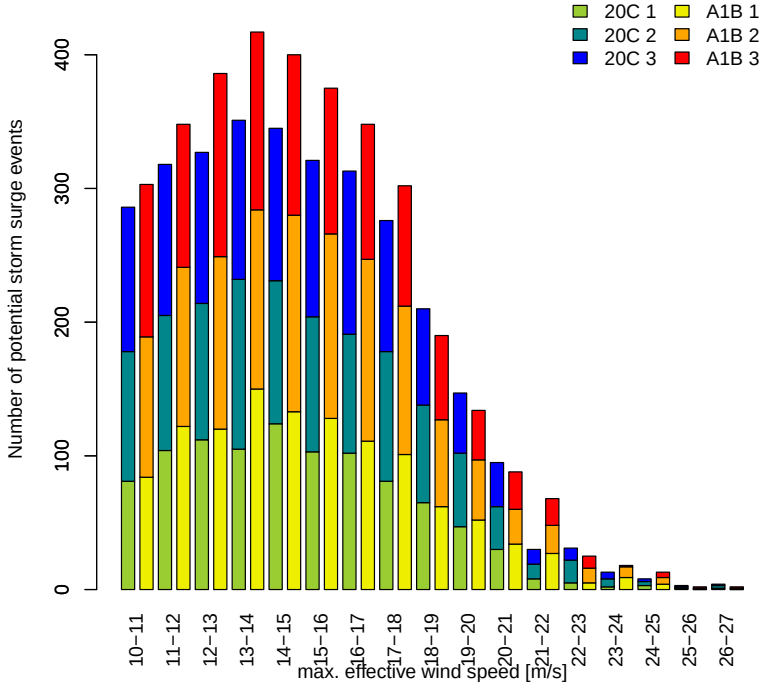

Figure 5. Number of potential storm surge events with respect to their maximum effective wind speed over the German Bight region for the three ensemble members of the 20C (1901–2000, green to blue) and A1B (2001–2100, yellow to red) period.

NHESSD
2, 3935–3963, 2014

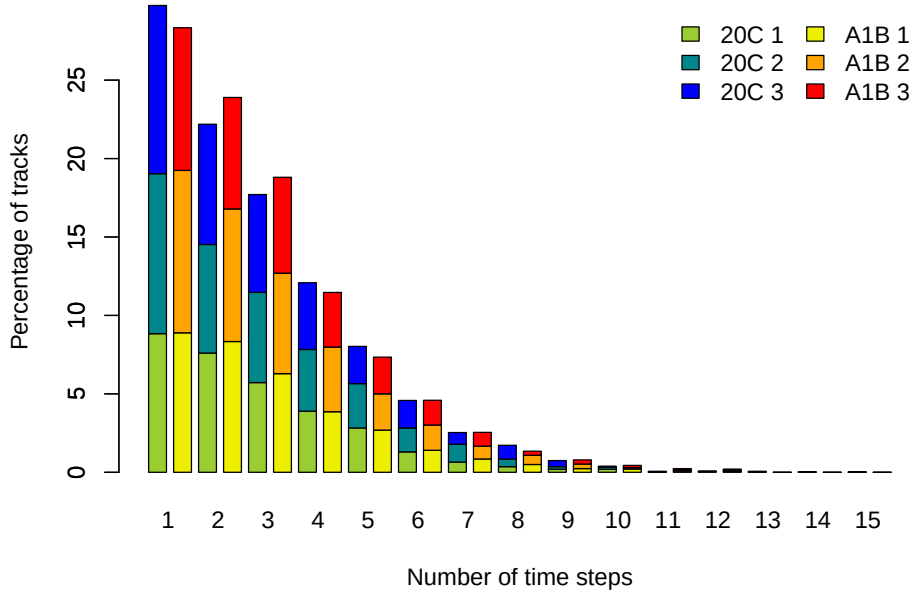

Figure 6. Number of potential storm surge events with respect to their number of time steps which exceed the critically effective wind speed for the three 20C runs (1901–2000, green to blue) and the three A1B runs (2001–2100, yellow to red).

NHESSD
2, 3935–3963, 2014

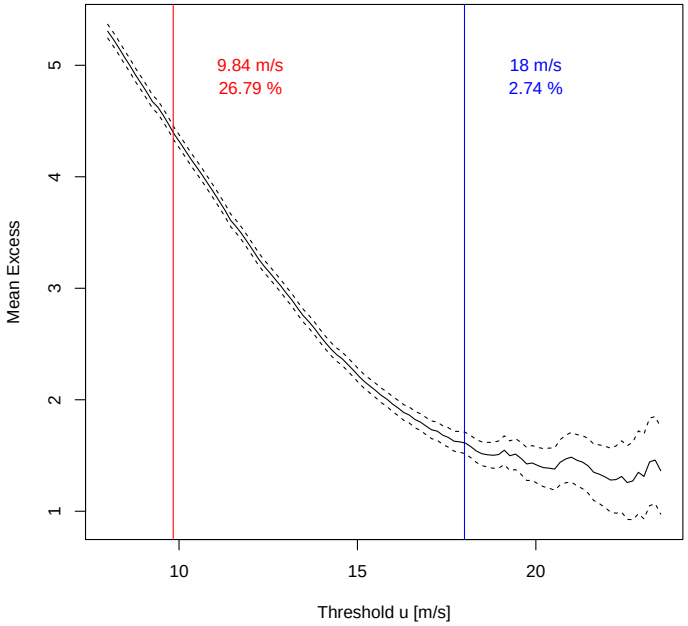

Figure 7. Mean residual life plot for the effective wind speed of all three 20C runs. The mean excess (continuous line) and the 95 % confidence intervals (dashed lines) are shown. Thresholds derived from historical storm surge events (red) and derived from the extreme value statistics (blue) are indicated as vertical lines. In addition the percentage of the exceeding is specified.

NHESSD
2, 3935–3963, 2014

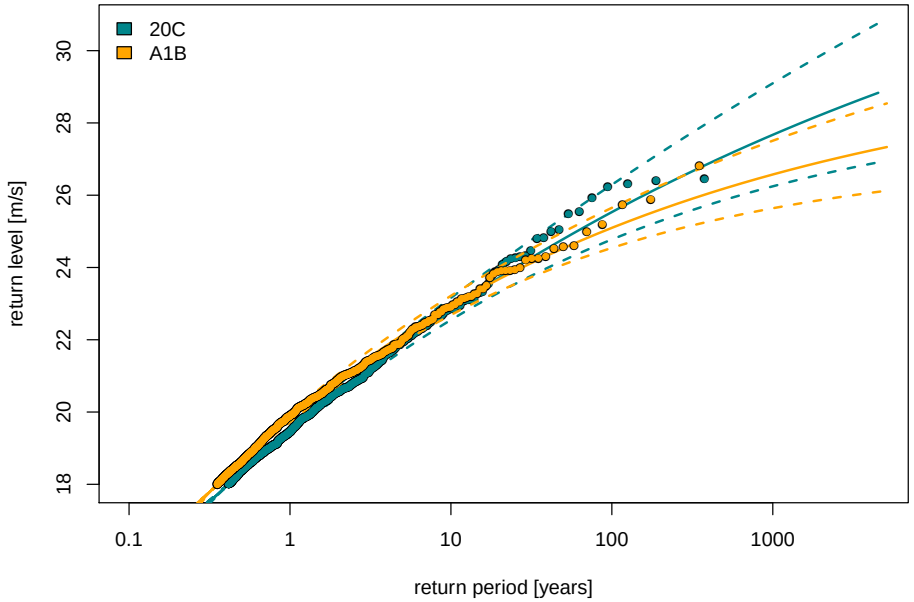

Figure 8. Return levels in $m\,s^{-1}$ (y axis) for different return periods in years (x axis) for 20C (1901–2000, turquoise) and A1B (2001–2100, orange) + the 95 % confidence intervals (dotted lines). Only effective wind speed values exceeding $18\,m\,s^{-1}$ are considered.

NHESSD
2, 3935–3963, 2014